JOURNAL OF MOLECULAR SPECTROSCOPY 131, 250–260 (1988)

New Observations of the $A\,^1\Pi_u$–$X\,^1\Sigma_g^+$ Transition (Phillips System) of C_2

M. DOUAY,[1] R. NIETMANN, AND P. F. BERNATH[2]

Department of Chemistry, University of Arizona, Tucson, Arizona 85721

We have reanalyzed the infrared part of the $A\,^1\Pi_u$–$X\,^1\Sigma_g^+$ (Phillips system) of C_2. Improved molecular constants were derived and the $v'' = 5$ and $v'' = 6$ vibrational levels of the $X\,^1\Sigma_g^+$ state were observed for the first time. RKR curves and $A\,^1\Pi_u$–$X\,^1\Sigma_g^+$ Franck–Condon factors were calculated from the equilibrium molecular constants.

I. INTRODUCTION

The C_2 molecule is found in a very wide variety of sources. C_2 occurs in comets (*1–3*), interstellar clouds (*4–11*), the sun (*12–14*), and in stellar atmospheres (*15, 16*). In the laboratory, C_2 is abundant in flames (*17–19*), explosions, and electrical discharges of carbon-containing molecules.

In 1948, Phillips (*20*) discovered the $A\,^1\Pi_u$–$X\,^1\Sigma_g^+$ electronic transition of C_2 which bears his name. Ballik and Ramsay (*21*) observed many additional bands of the Phillips system and in 1970 Marenin and Johnson provided a consistent set of spectroscopic constants (*22*). More recently, high-quality Fourier transform data for $^{12}C_2$ (*23, 24*), $^{12}C^{13}C$, and $^{13}C_2$ (*25*) have become available.

The oscillator strength of the $A\,^1\Pi_u$–$X\,^1\Sigma_g^+$ transition is still controversial with many experimental (*26–29*) and theoretical estimates (*30–33*). The A–X oscillator strength is relatively weak ($\sim 10^{-3}$). An accurate value is required to convert observed C_2 absorption spectra into an estimate of C_2 concentration (or, more precisely, into a C_2 column density).

The classic work of Ballik and Ramsey (*34*) proved the ground state of C_2 to be $X\,^1\Sigma_g^+$ rather than $a\,^3\Pi_u$ by the observation of singlet–triplet perturbations. As a result, there have been several ab initio studies of the interaction between the singlet and triplet manifolds (*35–37*). These perturbations have important astrophysical consequences because they (along with quadrupole radiation) permit the homonuclear C_2 molecule to relax and cool (*37*). Additional ab initio calculations of the molecular properties of C_2 have been carried out by many workers (*38–43*).

Many molecules fragment upon absorption of ultraviolet radiation or multiphoton absorption of visible or infrared photons, usually releasing simple molecules such as CN, CH, and C_2. The photochemical production of C_2 provides a convenient molecular

[1] Present address: Lab. de Spectroscopie des Molécules Diatomiques, CNRS UA779, Université des Sciences et Techniques de Lille, Bât. P5, 59655 Villeneuve d'Ascq Cedex, France.

[2] Alfred P. Sloan Fellow; Camille and Henry Dreyfus Teacher–Scholar.

0022-2852/88 $3.00

source for the study of C_2 reaction kinetics, C_2 quenching and C_2 triplet–singlet interconversion (*44–51*). C_2 is also formed in the reaction of hydrocarbons with rare gas metastables (*52*).

In the course of our discovery of the $B^1\Delta_g$–$A^1\Pi_u$ and $B'^1\Sigma_g^+$–$A^1\Pi_u$ electronic transitions (*53*) by infrared Fourier transform emission spectroscopy, we noted many previously unobserved bands of the Phillips system. A simultaneous fit of all of our observed singlet C_2 data has provided improved spectroscopic constants for $v = 0$–5 of the $A^1\Pi_u$ state and $v = 0$–6 of the $X^1\Sigma_g^+$ state. The $v = 5$ and 6 levels of the $X^1\Sigma_g^+$ state were not directly observed in any previous work.

II. EXPERIMENTAL DETAILS

Strong emission spectra of the C_2 molecule were found in two data sets previously recorded for other purposes. These spectra were excited by an electrodeless microwave discharge of hydrocarbons in a quartz tube. In one run a mixture of 2.75 Torr of He, 0.030 Torr of CH_4, and 0.040 Torr of white phosphorous vapor flowed through the discharge tube. The phosphorous is, presumably, not required. The second spectrum was recorded from a discharge of 3.3 Torr of argon and 0.80 Torr of allene. The first spectrum was extremely rich with strong spectra of CO, CH, PH, CP, P_2, ArH, and CN, as well as C_2. The second data set had a reduced signal-to-noise ratio for C_2, but was not as congested.

The emission from the discharge tube was observed with the McMath Fourier transform spectrometer of the National Solar Observatory at Kitt Peak. InSb detectors and a silicon filter limited the band pass to approximately 1800–9000 cm^{-1}. The unapodized resolution was set to 0.02 cm^{-1}. In the first spectrum, 10 scans were coadded in 70 min of integration, while in the second spectrum 8 scans were recorded in 58 min.

The first spectrum was calibrated with the vibration–rotation lines of the impurity molecule CO (*54*) near 2200 cm^{-1}. The calibration factor of $1 + 5.74 \times 10^{-7}$ was applied to the entire spectrum. The CO lines were much weaker in the second spectrum so the calibration was transferred to this spectrum using several strong lines of the 0–0 band of the $b^3\Sigma_g^-$–$a^3\Pi_u$ (Ballik–Ramsay) system. The absolute accuracy of the calibration is estimated to be better than ± 0.001 cm^{-1} for both spectra. The precision of the strong, unblended lines in the 0–0 band of the $A^1\Pi_u$–$X^1\Sigma_g^+$ transition is about 0.0002 cm^{-1}.

III. RESULTS AND DISCUSSION

The interferograms were transformed by G. Ladd to provide the two spectra. The line positions were extracted from the spectrum with the data reduction program DECOMP developed at Kitt Peak. The peak positions were found by fitting a Voigt lineshape function to each feature using a nonlinear least-squares procedure. Since the spectra are very congested, we proceeded initially by predicting the line positions and then picking out and assigning just a few lines. The preliminary fit of these lines provided an accurate prediction of the remaining lines in the band. Our search for new bands was guided by a preliminary Franck–Condon calculation.

TABLE I

Observed Line Positions of the $A^1\Pi_u$–$X^1\Sigma_g^+$ Transition of C_2 (in cm^{-1})

A. 0-0 BAND

J	R_{ee}	O-C	Q_{fe}	O-C	P_{ee}	O-C
0.0	8271.6056	-0				
2.0	8276.8191	1	8267.1726	0	8260.7396	1
4.0	8280.4061	-1	8264.3333	2	8251.4666	1
6.0	8282.3669	3	8259.8714	2	8240.5722	0
8.0	8282.6994	1	8253.7878	1	8228.0583	0
10.0	8281.4038	1	8246.0830	0	8213.9269	0
12.0	8278.4795	0	8236.7582	0	8198.1807	6
14.0	8273.9266	1	8225.8142	-1	8180.8197	-3
16.0	8267.7443	-3	8213.2523	-1	8161.8490	-3
18.0	8259.9336	-5	8199.0740	-1	8141.2704	-2
20.0	8250.4952	-2	8183.2802	-6	8119.0867	-1
22.0	8239.4286	-3	8165.8743	-2	8095.3009	-1
24.0	8226.7351	-3	8146.8568	-1	8069.9169	5
26.0	8212.4155	-4	8126.2304	0	8042.9385	22
28.0	8196.4721	7	8103.9973	1	8014.3634	-9
30.0	8178.9025	-5	8080.1601	3	7984.2025	-19
32.0	8159.7124	1	8054.7211	2	7952.4617	12
34.0	8138.9017	2	8027.6835	1	7919.1368	1
36.0	8116.4717	1	7999.0509	7	7884.2379	6
38.0	8092.4246	-3	7968.8243	-4	7847.7672	4
40.0	8066.7643	5	7937.0107	2	7809.7297	-3
42.0	8039.4912	7	7903.6094	-13	7770.1309	-9
44.0	8010.6136	60	7868.6190	-105		
46.0			7832.0705	-3		

B. 3-3 BAND

J	R_{ee}	O-C	Q_{fe}	O-C	P_{ee}	O-C
0.0	7554.2441	5				
2.0	7559.2771	0			7543.7117	2
4.0	7562.7194	2	7547.1599	3	7534.7033	-8
6.0	7564.5690	1	7542.7925	0	7524.1099	-3
8.0	7564.8257	3	7536.8382	0	7511.9314	0
10.0	7563.4881	-3	7529.2981	5	7498.1699	-1
12.0	7560.5577	-2	7520.1725	6	7482.8282	-1
14.0	7556.0320	-19	7509.4630	6	7465.9089	0
16.0	7549.9270	104	7497.1706	0	7447.4143	-2
18.0	7542.2061	-4	7483.3001	16	7427.3485	1
20.0	7532.9025	-20	7467.8482	4	7405.7129	-8
22.0	7522.0115	0	7450.8215	5	7382.5137	-3
24.0	7509.5273	-15	7432.2214	8	7357.7558	25
26.0	7495.4581	3	7412.0495	3	7331.4311	-40
28.0	7479.8013	11	7390.3122	24	7303.5632	-8
30.0	7462.5594	15	7367.0049	-6	7274.1441	-2
32.0	7443.7337	6	7342.1395	-4	7243.1832	23
34.0			7315.7149	-17		
36.0			7287.7392	-3		
38.0			7258.2131	4		
40.0			7227.1403	-1		

C. 4-4 BAND

J	R_{ee}	O-C	Q_{fe}	O-C	P_{ee}	O-C
0.0	7325.7597	-25				
2.0	7330.7399	1	7321.4922	-132	7315.3461	-10
4.0	7334.1431	-1	7318.7577	9	7306.4404	5

C. 4-4 BAND

J	R_{ee}	O-C	Q_{fe}	O-C	P_{ee}	O-C
6.0	7335.9723	4	7314.4382	3	7295.9637	2
8.0	7336.2253	1	7308.5496	1	7283.9197	-2
10.0	7334.9031	4	7301.0927	0	7270.3116	0
12.0	7332.0042	-1	7292.0689	4	7255.1419	12
14.0	7327.5294	-11	7281.4786	0	7238.4099	-3
16.0	7321.4922	105	7269.3249	2	7220.1219	-12
18.0	7313.8580	-5	7255.6089	1	7200.2836	7
20.0	7304.6618	-4	7240.3316	-16	7178.8926	-2
22.0	7293.8941	1	7223.5008	1	7155.9565	-4
24.0	7281.5596	40	7205.1139	-1	7131.4815	19
26.0	7267.6490	2	7185.1763	-2	7105.4660	9
28.0	7252.1755	-5	7163.6923	6		
30.0	7235.1517	118	7140.6603	-30		
32.0	7216.5427	-5	7116.0965	7		

D. 5-5 BAND

J	R_{ee}	O-C	Q_{fe}	O-C	P_{ee}	O-C
4.0	7113.0467	6			7085.6528	-31
6.0	7114.8674	6	7093.5760	-2	7075.3156	47
8.0	7115.1289	-58	7087.7705	-17	-	-
10.0	7113.8503	4	7080.4223	-3	7049.9910	11
12.0	7111.0128	2	7071.5322	31		
14.0	7106.6236	3	7061.0959	26		
16.0	-	-	-	-		
18.0	-	-	7035.6016	-27		
20.0	7084.1529	-14	-	-		
22.0	7073.5709	13	7003.9772	1		

E. 0-1 BAND

J	R_{ee}	O-C	Q_{fe}	O-C	P_{ee}	O-C
0.0	6444.1215	7				
2.0	6449.4433	1	6439.7967	-1	6433.3702	64
4.0	6453.2857	5	6437.2118	-1	6424.3452	-2
6.0	6455.6459	1	6433.1506	1	6413.8512	-2
8.0	6456.5250	5	6427.6128	0	6401.8833	-2
10.0	6455.9206	0	6420.5997	-2	6388.4437	-1
12.0	6453.8338	0	6412.1124	-2	6373.5340	-4
14.0	6450.2643	0	6402.1519	-1	6357.1578	0
16.0	6445.2118	0	6390.7195	-2	6339.3164	-1
18.0	6438.6765	-6	6377.8172	1	6320.0133	-2
20.0	6430.6602	-2	6363.4460	1	6299.2519	0
22.0	6421.1623	-2	6347.6088	6	6277.0347	0
24.0	6410.1841	-4	6330.3060	0	6253.3653	0
26.0	6397.7270	-3	6311.5419	0	6228.2479	2
28.0	6383.7919	-5	6291.3184	1	6201.6863	8
30.0	6368.3810	-3	6269.6382	1	6173.6837	9
32.0	6351.4959	0	6246.5039	-2	6144.2446	8
34.0	6333.1353	-25	6221.9195	-2	6113.3734	3
36.0	6313.3092	-3	6195.8886	3	6081.0760	7
38.0			6168.4131	0	6047.3540	-11
40.0			6139.4994	10	6012.2178	-1

Note. Observed minus calculated line positions are in units of 10^{-4} cm^{-1}.

[a] Perturbed.

TABLE I—*Continued*

F. 1-2 BAND

J	R_{ee}	O-C	Q_{fe}	O-C	P_{ee}	O-C
0.0	6228.9341	-1				
2.0	6234.1968	-4	6224.6534	2	6218.2882	0
4.0	6237.9924	3	6222.0888	-4	6209.3591	0
6.0	6240.3179	3	6218.0607	0	6198.9661	-2
8.0	6241.1732	0	6212.5680	-1	6187.1113	-4
10.0	6240.5577	-5	6205.6123	0	6173.7968	-5
12.0	6238.4727	0	6197.1943	0	6159.0251	-3
14.0	6234.9166	1	6187.3154	1	6142.7982	-4
16.0	6229.8902	3	6175.9772	3	6125.1196	0
18.0	6223.3936	3	6163.1809	2	6105.9914	0
20.0	6215.4276	1	6148.9289	2	6085.4173	2
22.0	6205.9932	0	6133.2235	4	6063.4002	1
24.0	6195.0919	0	6116.0654	-8	6039.9452	9
26.0	6182.7250	0	6097.4613	3	6015.0558	23
28.0	6168.8930	-9	6077.4100	-2	5988.7322	2
30.0	6153.5973	-36	6055.9171	-1	5960.9839	-2
32.0	6136.8471	-11	6032.9867	12	5931.8146	-3
34.0	6118.6389	5	6008.6187	0	5901.2299	5
36.0	6098.9732	-9				
38.0	6077.8594	6				

G. 2-1 BAND

J	R_{ee}	O-C	Q_{fe}	O-C	P_{ee}	O-C
0.0	6018.7230	1				
2.0	6023.9295	9	6014.4833	-38		
4.0	6027.6775	-29	6011.9486	-1	5999.3524	-32
6.0	6029.9788	11	6007.9589	-13	5989.0687	-27
8.0	6030.8192	-2	6002.5221	-3	5977.3403	0
10.0	6030.2042	-15	5995.6368	6	5964.1654	12
12.0	6028.1375	12	5987.3081	55	5949.5447	-8
14.0	6024.6117	6	5977.5247	16	5933.4862	-8
16.0			5966.2992	0	5915.9945	27
18.0	6013.1731	-227[a]	5953.6331	0	5897.0705	79
20.0	6005.2821	-250[a]	5939.5284	16	5876.6788	-242[a]
22.0	5995.9619	-39	5923.9843	17	5854.8947	-220[a]
24.0	5985.1720	-12	5907.0021	-10	5831.7054	-21
26.0	5972.9314	3	5888.5895	-17	5807.0783	-10
28.0	5959.2387	-22				
30.0	5944.1048	-3				

H. 0-2 BAND

J	R_{ee}	O-C	Q_{fe}	O-C	P_{ee}	O-C
0.0	4644.9160	-61				
2.0	4650.3560	1	4640.7109	14	4634.2781	17
4.0	4654.4579	5	4638.3849	6	4625.5168	-8
6.0	4657.2258	-1	4634.7308	1	4615.4325	8
8.0	4658.6606	-3	4629.7490	-3	4604.0197	-3
10.0	4658.7619	0	4623.4411	-1	4591.2850	-1
12.0	4657.5290	5	4615.8072	0	4577.2286	-4
14.0	4654.9616	6	4606.8481	-6	4561.8537	-7
16.0	4651.0593	-1	4596.5664	-8	4545.1629	-11
18.0	4645.8238	-6	4584.9644	0	4527.1611	2
20.0	4639.2570	2	4572.0417	-4	4507.8476	-5
22.0	4631.3582	8	4557.8026	-2	4487.2290	-3
24.0	4622.1279	4	4542.2498	8	4465.3093	9
26.0	4611.5694	7	4525.3839	7	4442.0902	12
28.0	4599.6835	9	4507.2079	-5	4417.5723	-32

H. 0-2 BAND

J	R_{ee}	O-C	Q_{fe}	O-C	P_{ee}	O-C
30.0	4586.4703	-11	4487.7284	3	4391.7749	21
32.0	4571.9363	-11	4466.9447	-10		
34.0	4556.0844	11	4444.8645	-6		

I. 1-3 BAND

J	R_{ee}	O-C	Q_{fe}	O-C	P_{ee}	O-C
0.0	4458.9268	-14				
2.0	4464.3055	3	4454.7614	3	4448.3994	33
4.0	4468.3648	-3	4452.4615	-8	4439.7330	8
6.0	4471.1072	-3	4448.8515	8	4429.7556	-6
8.0	4472.5320	4	4443.9263	-3	4418.4703	1
10.0	4472.6370	-1	4437.6914	1	4405.8760	-2
12.0	4471.4260	18	4430.1464	6	4391.9781	11
14.0	4468.8941	12	4421.2925	8	4376.7746	-4
16.0	4465.0450	13	4411.1312	5	4360.2740	5
18.0	4459.8779	4	4399.6662	14	4342.4758	3
20.0	4453.3962	11	4386.8975	12	4323.3853	7
22.0	4445.5988	10	4372.8282	6	4303.0066	20
24.0	4436.4802	-69	4357.4604	-10	4281.3398	3
26.0	4426.0628	-22	4340.8003	-7	4258.3929	-5
28.0	4414.3366	33	4322.8495	0	4234.1745	32
30.0	4401.2918	-25	4303.6088	-17	4208.6761	-13
32.0	4386.9515	9	4283.0860	-18		
34.0	4371.3079	29	4261.2951	97		

J. 2-4 BAND

J	R_{ee}	O-C	Q_{fe}	O-C	P_{ee}	O-C
0.0	4279.0606	-7				
2.0	4284.3848	7	4274.9421	-5	4268.6500	37
4.0	4288.4090	0	4272.6770	-3	4260.0790	-52
6.0	4291.1404	50	4269.1178	-2	4250.2268	-24
8.0	4292.5617	-9	4264.2655	0	4239.0832	-2
10.0	4292.6893	-13	4258.1212	1	4226.6497	6
12.0	4291.5187	-7	4250.6914	57	4212.9274	-13
14.0	4289.0500	7	4241.9602	-10	4197.9259	6
16.0	4285.2839	29	4231.9492	-2	4181.6420	1
18.0	4280.1926	-227[a]	4220.6533	6	4164.0852	31
20.0	4273.8339	-198[a]	4208.0735	1	4145.2261	-234[a]
22.0	4266.1971	-5	4194.2156	12	4125.1303	-182[a]
24.0	4257.2496	5	4179.0770	-18	4103.7819	-13
26.0	4247.0090	-10	4162.6694	-8	4081.1585	0
28.0	4235.4825	-7	4144.9936	12	4057.2777	-18
30.0	4222.6778	62	4126.0477	-16	4032.1511	-4
32.0			4105.8466	8	4005.7780	-24

K. 3-5 BAND

J	R_{ee}	O-C	Q_{fe}	O-C	P_{ee}	O-C
2.0	4112.0800	-5	4102.7372	-51	4096.5259	111
4.0	4116.0783	-1	4100.5193	5	4088.0628	-6
6.0	4118.8023	5	4097.0252	-1	4078.3452	20
8.0	4120.2499	-3	4092.2636	6	4067.3612	48

TABLE I—*Continued*

K. 3-5 BAND

J	R_{ee}	O-C	Q_{fe}	O-C	P_{ee}	O-C
10.0	4120.4248	9	4086.2336	6	4055.1064	9
12.0	4119.3235	5	4078.9367	-2	4041.5932	-1
14.0	4116.9476	-7	4070.3791	22	4026.8178	-54
16.0	4113.3017	7	4060.5546	-4	-	-
18.0	4108.3768	-55	4049.4751	9	3993.5249	7
20.0	4102.1952	11	4037.1381	7	3975.0044	11
22.0	4094.7458	74[a]	4023.5510	32[a]	3955.2435	26[a]
24.0	4086.0323	147[a]	4008.7254	161[a]	3934.2569	149[a]
26.0	4076.1067	721[a]	3992.6941	682[a]	3912.0813	694[a]
28.0	4064.5810	-2113[a]	3975.0886	-2133[a]	3888.3297	-2265[a]

L. 4-6 BAND

J	R_{ee}	O-C	Q_{fe}	O-C
2.0	3949.3819	48		
4.0	-	-	3937.9763	-59
6.0	3956.1219	21	3934.5862	5
8.0	3957.6254	-12	3929.9467	-43
10.0	3957.8876	20	3924.0778	22
12.0	3956.9353	436[a]	3917.0017	459[a]
14.0	3954.4797	-1597[a]	3908.4288	-1587[a]
16.0	3951.1233	4[a]	3898.9650	-8[a]

In the end, 12 bands were identified and analyzed: 0–0, 3–3, 4–4, 5–5, 0–1, 1–2, 2–3, 0–2, 1–3, 2–4, 3–5, and 4–6. The 3–3, 4–4, 5–5, 3–5, and 4–6 bands are new. The observation of bands in the Phillips system with $v'' = 5$ and 6 provides accurate constants for these high-lying vibrational levels of the ground state. The observed line positions and rotational assignments are provided in Table I.

The lines of Table I and all of the observed lines of $B^1\Delta_g$–$A^1\Pi_u$ and $B'^1\Sigma_g^+$–$A^1\Pi_u$ were fitted simultaneously with the customary energy level expression for each vibration level in each electronic state:

$$T_v + B_vJ(J+1) - D_v[J(J+1)]^2 + H_v[J(J+1)]^3 \pm \delta_{1\Lambda}J(J+1)[q_v + q_{Dv}J(J+1)]/2.$$

TABLE II

Molecular Constants for the $X^1\Sigma_g^+$ State of C_2 (in cm^{-1})

Constant	v=0	v=1	v=2	v=3	v=4	v=5	v=6
T_v	0.0	1827.4849(2)	3626.6835(2)	5396.6892(4)	7136.3507(6)	8844.1241(11)	10517.9659(39)
B_v	1.8110717(21)[a]	1.7928789(21)	1.7743392(23)	1.7553998(26)	1.7358967(47)	1.7157027(135)	1.693813(78)
$10^6 \times D_v$	7.00315(118)	7.05398(117)	7.0944(24)	7.2066(21)	7.2941(90)	7.499(31)	4.73(25)
$10^{11} \times H_v$	-	-	-1.452(133)	-	-1.78(55)	-	-

[a] The numbers in parentheses are one standard deviation in the last digit.

TABLE III

Molecular Constants for the $A^1\Pi_u$ State of C_2 (in cm^{-1})

Constant	v=0	v=1	v=2	v=3	v=4	v=5
T_v	8268.38962(15)[a]	9852.4355(2)	11412.2643(4)	12947.8195(5)	14459.0343(7)	15945.8285(23)
B_v	1.6081345(20)	1.5910931(22)	1.5739723(30)	1.5567609(30)	1.5394486(41)	1.522047(25)
$10^6 \times D_v$	6.52569(114)	6.53614(145)	6.5731(28)	6.6026(24)	6.6289(38)	6.657(48)
$10^4 \times q_v$	-1.9573(34)	-1.9265(25)	-1.8813(55)	-1.8731(70)	-1.8659(89)	-1.847(75)
$10^9 \times q_{Dv}$	5.08(27)	-	-	-	-	-

[a] The numbers in parentheses are one standard deviation in the last digit.

Approximate weights were chosen for each line on the basis of the signal-to-noise ratio, as well as freedom from blending or perturbations. The energy origin of this fit was $v = 0$, $J = 0$ of the $X^1\Sigma_g^+$ state and Λ-doubling was included only for the $A^1\Pi_u$ state. The spectroscopic constants for the $X^1\Sigma_g^+$ and $A^1\Pi_u$ states are reported in Tables II and III.

The constants of Tables II and III were converted to equilibrium molecular constants (Table IV) using the expressions

$$G(v) = \omega_e(v + \tfrac{1}{2}) - \omega_e x_e(v + \tfrac{1}{2})^2 + \omega_e y_e(v + \tfrac{1}{2})^3 + \omega_e z_e(v + \tfrac{1}{2})^4 + \omega_e a_e(v + \tfrac{1}{2})^5$$

$$B_v = B_e - \alpha_e(v + \tfrac{1}{2}) + \gamma_e(v + \tfrac{1}{2})^2 + \delta_e(v + \tfrac{1}{2})^3$$

TABLE IV

Equilibrium Molecular Constants for the $X^1\Sigma_g^+$ and $A^1\Pi_u$ States of C_2 (in cm^{-1})

State	ω_e	$\omega_e x_e$	$\omega_e y_e$	$\omega_e z_e$	$\omega_e a_e$
$X^1\Sigma_g^+$	1855.0142(129)[a]	13.5547(124)	-0.1321(50)	0.00357(89)	-0.001116(57)
$A^1\Pi_u$	1608.1990(52)	12.0597(27)	-0.010555(39)	-	-
	B_e	α_e	$\gamma_e \times 10^{-5}$	$\delta_e \times 10^{-5}$	
$X^1\Sigma_g^+$	1.820099(37)	0.018012(63)	-6.33(286)	-2.06(37)	
$A^1\Pi_u$	1.6166275(27)	0.0169691(51)	-3.34(25)	-0.154(33)	
	$D_e \times 10^{-6}$	$\beta_e \times 10^{-8}$	T_e		
$X^1\Sigma_g^+$	6.9640(124)	6.41(69)	-		
$A^1\Pi_u$	6.5086(54)	2.53(29)	8391.4085(46)		
	$q_e \times 10^{-4}$	$\alpha_q \times 10^6$			
$A^1\Pi_u$	-1.9676(70)	2.74(37)			

[a] One standard deviation uncertainty in parentheses.

TABLE V

RKR Turning Points for the $X^1\Sigma^+$ State of C_2

v	E_v (cm^{-1})	R_{min} (Å)	R_{max} (Å)
0.0	923.9840	1.19052	1.30093
0.5	1841.2118	1.17072	1.32735
1.0	2751.4689	1.15615	1.34860
1.5	3654.6561	1.14428	1.36723
2.0	4550.6670	1.13413	1.38423
2.5	5439.3835	1.12519	1.40009
3.0	6320.6724	1.11717	1.41513
3.5	7194.3803	1.10988	1.42955
4.0	8060.3301	1.10317	1.44348
4.5	8918.3167	1.09696	1.45704
5.0	9768.1023	1.09117	1.47030
5.5	10609.4130	1.08575	1.48334
6.0	11441.9340	1.08064	1.49621

$$D_v = D_e + \beta_e(v + \tfrac{1}{2})$$

$$q_v = q_e + \alpha_q(v + \tfrac{1}{2}).$$

The large number of expansion constants required for the B_v and $G(v)$ expansions (Table IV) is probably a reflection of the global perturbations and interactions among the low-lying states of C_2.

The B_v and $G(v)$ expansions were input to an RKR program to calculate the classical turning points (Tables V and VI) of the $X^1\Sigma_g^+$ and $A^1\Pi_u$ potential curves. Figure 1 is a plot of the potential energy curves of the low-lying $X^1\Sigma_g^+$, $A^1\Pi_u$, $B^1\Delta_g$, and

TABLE VI

RKR Turning Points of the $A^1\Pi_u$ State of C_2

v	E_v (cm^{-1})	R_{min} (Å)	R_{max} (Å)
0.0	801.1033[a]	1.26266	1.38925
0.5	1596.1488	1.24151	1.40975
1.0	2385.1486	1.22597	1.43269
1.5	3168.0948	1.21333	1.45280
2.0	3944.9795	1.20253	1.47112
2.5	4715.7947	1.19302	1.48822
3.0	5480.5326	1.18449	1.50439
3.5	6239.1853	1.17674	1.51986
4.0	6991.7448	1.16961	1.53476
4.5	7738.2031	1.16301	1.54921
5.0	8478.5525	1.15685	1.56329

[a] Relative to the bottom of the $A^1\Pi_u$ well. To convert the origin of the E_v scale to the bottom of the $X^1\Sigma_g^+$ well, 8391.2703 cm^{-1} must be added. This number was calculated using the experimental value of 8268.3896 cm^{-1} for T_{oo}. Note that these potential curves include the Dunham Y_{oo} correction.

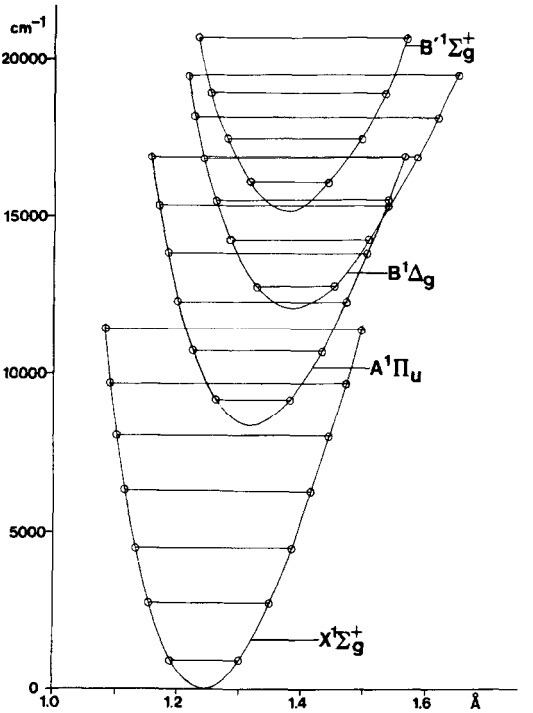

FIG. 1. The RKR potential curves of the low-lying singlet states of C_2.

$B'^1\Sigma_g^+$ states of C_2 as determined from our RKR turning points. The $A^1\Pi_u$ and $X^1\Sigma_g^+$ potential energy curves were used to calculate the A–X Franck–Condon factors (Table VII). We found all of the bands expected on the basis of intensity estimates from the Franck–Condon factors of Table VII.

The B_e values of Table IV result in r_e values of 1.242440 and 1.318311 Å for the $X^1\Sigma_g^+$ and $A^1\Pi_u$ states, respectively.

The spectroscopic constants of Tables II and III are the most useful result of our reanalysis of the Phillips system. For example, the 2–0 band near 8760 Å is observed in absorption in interstellar clouds (*5–11*). Although we have not directly observed the 2–0 band, the line positions of this band, calculated with the constants of Tables II and III, should be more accurate than the previous measurements. In general, our spectroscopic constants and line positions are in agreement with, but more accurate than, the previous measurements.

The line positions of Table I display three perturbations (Table VIII). In the 2–4 and 2–3 bands, the e parity level of $v' = 2$ of $A^1\Pi_u$ with $J' = 19, 21$ is perturbed by the corresponding J's (F_2, $N = 19, 21$) e parity level of $v = 1$ of the $c^3\Sigma_u^+$ state. This perturbation was predicted by Chauville *et al.* (*23*), and also observed by Davis *et al.* (*24*). This perturbation, along with others previously observed, allowed Davis *et al.* (*24*) to calculate improved spectroscopic constants for the $c^3\Sigma_u^+$ state.

In the 3–5 band, the $J'' = 22, 24, 26$, and 28 e parity levels of $v'' = 5$ of the $X^1\Sigma_g^+$ state are perturbed by $v = 2$ of the $b^3\Sigma_g^-$ state. In the 4–6 band the $J'' = 12, 14$ e levels

TABLE VII

$A^1\Pi_u$–$X^1\Sigma_g^+$ Franck–Condon Factors

v' \ v''	0	1	2	3	4	5	6
0	0.412E0	0.398E0	0.155E0	0.311E-1	0.338E-2	0.184E-3	0.343E-5
1	0.332E0	0.553E-2	0.289E0	0.272E0	0.883E-1	0.131E-1	0.859E-3
2	0.162E0	0.172E0	0.578E-1	0.116E0	0.305E0	0.155E0	0.301E-1
3	0.630E-1	0.200E0	0.318E-1	0.142E0	0.184E-1	0.271E0	0.216E0
4	0.215E-1	0.126E0	0.138E0	0.116E-2	0.155E0	0.162E-2	0.204E0
5	0.684E-2	0.601E-1	0.145E0	0.578E-1	0.358E-1	0.115E0	0.302E-1

of $v'' = 6$ of the $X^1\Sigma_g^+$ state are perturbed by $v = 3$ of the $b^3\Sigma_g^-$ state. The corresponding perturbations were observed by Roux *et al.* (*55*) in the $b^3\Sigma_g^-$–$a^3\Pi_u$ Ballik–Ramsay system. The shifts in $v = 5$, $J = 26$ and 28 for the $X^1\Sigma_g^+$ state predicted by Roux *et al.* (*55*) are 0.101 and -0.171 cm^{-1} compared to our values (Table VIII) of 0.070 and -0.217 cm^{-1}, respectively. For $v = 6$ of the $X^1\Sigma_g^+$ state, the predictions of Roux *et al.* are +0.074 and -0.127, while our values are 0.045 and -0.159 cm^{-1} for $J = 12$ and 14, respectively. The agreement is reasonable, but not perfect, between the two sets of measurements. The discrepancies are presumably caused by systematic, model-dependent errors in the prediction of the unperturbed line positions. The observation of level shifts equal in magnitude (but opposite in sign) by us and by Roux *et al.* (*55*) confirms the two sets of assignments.

TABLE VIII

Observed Perturbations in the $A^1\Pi_u$–$X^1\Sigma_g^+$ System of C_2 (in cm^{-1})

Perturbed State	Perturbing State	Band	Line	Obs.-Calc	Line	Obs.-Calc.	Line	Obs.-Calc.
		3 - 5	R(22)	0.0074	Q(22)	0.0032	P(22)	0.0026
v=5	v=2		R(24)	0.0147	Q(24)	0.0161	P(24)	0.0149
$X^1\Sigma_g^+$	$b^3\Sigma_g^-$		R(26)	0.0721	Q(26)	0.0682	P(26)	0.0694
			R(28)	-0.2113	Q(28)	-0.2133	P(28)	-0.2265
v=6	v=3	4 - 6	R(12)	0.0436	Q(12)	0.0459	-	
$X^1\Sigma_g^+$	$b^3\Sigma_g^-$		R(14)	-0.1597	Q(14)	-0.1587	-	
		2 - 4	R(18)	-0.0227	-		P(20)	-0.0234
v=2	v=1		R(20)	-0.0198	-		P(22)	-0.0182
$A^1\Pi_u$	$c^3\Sigma_u^+$	2 - 3	R(18)	-0.0227	-		P(20)	-0.0242
			R(20)	-0.0250	-		P(22)	-0.0220

CONCLUSION

We have reanalyzed the $A^1\Pi_u$–$X^1\Sigma_g^+$ Phillips system of C_2 and have observed several new vibrational bands. The $v'' = 5$ and 6 levels of the $X^1\Sigma_g^+$ state were observed for the first time. Since C_2 is such a ubiquitous molecule, our improved spectroscopic constants should prove useful.

ACKNOWLEDGMENTS

The National Solar Observatory is operated by the Association of Universities for Research in Astronomy, Inc., under contract with the National Science Foundation. We thank J. Wagner, R. Ram, and G. Ladd for assistance in acquiring our C_2 spectrum. Acknowledgment is made to the donors of the Petroleum Research Fund, administered by the American Chemical Society, for partial support of this work. Some support was also provided by the Air Force Astronautics Laboratory Grant No. F04611-87-K-0020.

RECEIVED: May 16, 1988

REFERENCES

1. P. MAYER AND C. R. O'DELL, *Astrophys. J.* **153,** 951–962 (1968).
2. J. R. JOHNSON, U. FINK, AND H. P. LARSON, *Astrophys. J.* **270,** 769–777 (1983).
3. D. L. LAMBERT AND A. C. DANKS, *Astrophys. J.* **268,** 428–446 (1983).
4. S. P. SOUZA AND B. L. LUTZ, *Astrophys. J.* **216,** L49–L51 (1977).
5. F. H. CHAFFEE, JR., AND B. L. LUTZ, *Astrophys. J.* **221,** L91–L93 (1978).
6. L. M. HOBBS, *Astrophys. J.* **232,** L175–L177 (1979).
7. L. M. HOBBS AND B. CAMBELL, *Astrophys. J.* **254,** 108–110 (1982).
8. F. H. CHAFFEE, JR., B. L. LUTZ, J. H. BLACK, P. A. VANDEN BOUT, AND R. L. SNELL, *Astrophys. J.* **236,** 474–480 (1980).
9. L. M. HOBBS, *Astrophys. J.* **243,** 485–488 (1981).
10. E. F. VAN DISHOECK AND T. DE ZEEUW, *Mon. Not. R. Astron. Soc.* **206,** 383–406 (1984).
11. L. M. HOBBS, J. H. BLACK, AND E. F. VAN DISHOECK, *Astrophys J.* **271,** L95–L99 (1983).
12. N. GREVESSE AND A. J. SAUVAL, *Astron. Astrophys.* **27,** 29–43 (1973).
13. J. W. BRAULT, L. DELBOUILLE, N. GREVESSE, G. ROLAND, A. J. SAUVAL, AND L. TESTERMAN, *Astron. Astrophys.* **108,** 201–205 (1982).
14. D. L. LAMBERT, *Mon. Not. R. Astron. Soc.* **182,** 249–272 (1978).
15. F. QUERCI, M. QUERCI, AND V. G. KUNDE, *Astron. Astrophys.* **15,** 256–274 (1971).
16. J. H. GOEBEL, J. D. BREGMAN, D. M. COOPER, D. GOORVITCH, S. R. LANGHOFF, AND F. C. WITTEBORN, *Astrophys. J.* **270,** 190–199 (1983).
17. R. BLEEKRODE AND W. C. NIEUWPOORT, *J. Chem. Phys.* **43,** 3680–3687 (1965).
18. A. G. GAYDON AND H. G. WOLFHARD, "Flames," Chapman & Hall, London, 1978.
19. J. A. BARNARD AND J. N. BRADLEY, "Flame and Combusion," 2nd ed., Chapman & Hall, London, 1985.
20. J. G. PHILLIPS, *Astrophys. J.* **107,** 389–399 (1948).
21. E. A. BALLIK AND D. A. RAMSAY, *Astrophys. J.* **137,** 84–101 (1963).
22. I. R. MARENIN AND H. R. JOHNSON, *J. Quant. Spectrosc. Radiat. Transfer* **10,** 305–309 (1970).
23. J. CHAUVILLE, J. P. MAILLARD, AND A. W. MANTZ, *J. Mol. Spectrosc.* **68,** 309–411 (1977).
24. S. P. DAVIS, M. C. ABRAMS, J. G. PHILLIPS, AND M. L. P. RAO, *J. Opt. Soc. Amer. B,* in press.
25. C. AMIOT AND J. VERGES, *Astron. Astrophys. Suppl.* **51,** 257–265 (1983).
26. F. ROUX, D. CERNY, AND J. D'INCAN, *Astrophys. J.* **204,** 940 (1976).
27. P. ERMAN, D. L. LAMBERT, M. LARSSON, AND B. MANNFORS, *Astrophys. J.* **253,** 983–988 (1982).
28. S. P. DAVIS, W. H. SMITH, J. W. BRAULT, R. PECYNER, AND J. WAGNER, *Astrophys. J.* **287,** 455–460 (1984).
29. W. BAUER, K. H. BECKER, C. HUBRICH, R. MEUSER, AND J. WILDT, *Astrophys. J.* **296,** 758–764 (1985).
30. E. F. VAN DISHOECK, *Chem. Phys.* **77,** 277–286 (1983).

31. C. F. CHABALOWSKI, S. D. PEYERIMHOFF, AND R. J. BUENKER, *Chem. Phys.* **81,** 57–72 (1983).
32. G. THEODORAKOPOULOS, I. D. PETSALAKIS, C. A. NICOLAIDES, AND R. J. BUENKER, *Chem. Phys.* **112,** 319–324 (1987).
33. S. V. O'NEIL, P. ROSMUS, AND H. J. WERNER, *J. Chem. Phys.* **87,** 2847–2853 (1987).
34. E. A. BALLIK AND D. A. RAMSAY, *Astrophys. J.* **137,** 61–83 (1963).
35. S. R. LANGHOFF, M. L. SINK, R. H. PRITCHARD, C. W. KERN, S. J. STRICKLER, AND M. J. BOYD, *J. Chem. Phys.* **67,** 1051–1060 (1977).
36. J. LE BOURLOT AND E. ROUEFF, *J. Mol. Spectrosc.* **120,** 157–168 (1986).
37. E. F. VAN DISHOECK AND J. H. BLACK, *Astrophys. J.* **258,** 533–547 (1982).
38. J. BARSUHN, *Z. Naturforsch., A* **27,** 1031–1041 (1972).
39. K. KIRBY AND B. LIU, *J. Chem. Phys.* **70,** 893–900 (1979).
40. B. POUILLY, J. M. ROBBE, J. SCHAMPS, AND E. ROUEFF, *J. Phys. B* **16,** 437–448 (1983).
41. J. A. NICHOLS AND J. SIMONS, *J. Chem. Phys.* **86,** 6972–6981 (1987).
42. C. W. BAUSCHLICHER, JR., AND S. R. LANGHOFF, *J. Chem. Phys.* **87,** 2919–2924 (1987).
43. C. M. ROHLFING AND R. L. MARTIN, *J. Phys. Chem.* **90,** 2043–2046 (1986).
44. C. T. LIN, PH. AVOURIS, AND Y. J. THEFAINE, *J. Phys. Chem.* **86,** 2271–2273 (1982).
45. W. M. PITTS, L. PASTERNACK, AND J. R. MCDONALD, *Chem. Phys.* **68,** 417–422 (1982).
46. L. PASTERNACK, W. M. PITTS, AND J. R. MCDONALD, *Chem. Phys.* **57,** 19–28 (1981).
47. W. L. FAUST, L. S. GOLDBERG, B. B. CRAIG, AND R. G. WEISS, *Chem. Phys. Lett.* **83,** 265–269 (1981).
48. V. M. DONNELLY AND L. PASTERNACK, *Chem. Phys.* **39,** 427–432 (1979).
49. W. HACK AND W. LANGEL, *Chem. Phys. Lett.* **81,** 387–390 (1981).
50. M. H. YU, M. R. LEVY, AND C. WITTIG, *J. Chem. Phys.* **72,** 3789–3795 (1980).
51. H. REISLER, M. MANGIR, AND C. WITTIG, *J. Chem. Phys.* **71,** 2109–2117 (1979); **73,** 829–835 (1980); **73,** 2280–2286 (1980); *Chem. Phys.* **47,** 49–58 (1980).
52. D. H. WINICUR AND J. L. HARDWICK, *Chem. Phys.* **94,** 157–166 (1985).
53. M. DOUAY, R. NIETMANN, AND P. F. BERNATH, *J. Mol. Spectrosc.* **131,** 261–271 (1988).
54. L. R. BROWN AND R. A. TOTH, *J. Opt. Soc. Amer. B* **2,** 842–856 (1985).
55. F. ROUX, G. WANNOUS, F. MICHAUD, AND J. VERGES, *J. Mol. Spectrosc.* **109,** 334–344 (1985).